Competition between valence and spin fluctuations in the vicinity of the quantum critical point of the heavy fermion compound $YbAuCu_4$

2008 J. Phys.: Condens. Matter 20 175201

(http://iopscience.iop.org/0953-8984/20/17/175201)

J. Phys.: Condens. Matter **20** (2008) 175201 (8pp) doi:10.1088/0953-8984/20/17/175201

Competition between valence and spin fluctuations in the vicinity of the quantum critical point of the heavy fermion compound $YbAuCu_4$

S Wada[1], A Yamamoto[1,4], K Ishida[2] and J L Sarrao[3]

[1] Department of Physics, Graduate School of Science, Kobe University, Kobe 657-8501, Japan
[2] Department of Physics, Graduate School of Science, Kyoto University, Kyoto 606-8502, Japan
[3] Los Alamos National Laboratory, Mail Stop G754, Los Alamos, NM 87545, USA

Received 18 January 2008, in final form 10 March 2008
Published 1 April 2008
Online at stacks.iop.org/JPhysCM/20/175201

Abstract

The quantum criticality of the Yb-based heavy fermion compound $YbAuCu_4$ with noninteger valence close to unity has been investigated through low-temperature resistivity, magnetization, and nuclear magnetic resonance measurements in several fixed magnetic fields H. We found that, with increasing H, $YbAuCu_4$ is driven from the originally antiferromagnetically ordered ground state (Néel temperature $T_N \sim 0.9$ K) to a nonmagnetic Fermi liquid one through the field-tuned quantum critical point (QCP) at $H_{cr} \simeq 13$ kOe. The experimental results also provide the first evidence that a crossover valence transition near the magnetic QCP is stabilized with the application of external field, in marked contrast to the destabilization of the first-order valence transition. The T–H phase diagram of $YbAuCu_4$ and the T–X phase diagram established for the $YbXCu_4$ (X = Pd, Au, Cu, Ag) series indicate that the evolution of valence fluctuations near the magnetic QCP quickly interacts with the critical spin fluctuations. We suggest that the competition between the Kondo temperature and crossover valence transition temperature is central to the long-standing puzzles of localized–itinerant duality and the extent of degeneracy in the crystal electric field ground state.

(Some figures in this article are in colour only in the electronic version)

1. Introduction

The intermediate valence in cerium and ytterbium compounds reflects the peculiar nature of the quasi-atomic 4f orbital and the quantum admixture of two electronic configurations corresponding to different electron occupations, $n_f = 1$ and 0, of the 4f shell, one electron being able to fluctuate between the localized 4f orbital and extended 5d–6s states. Much of the fundamental nature of the heavy Fermi liquid (HFL) state of cerium compounds has been clarified by the leading theoretical scenario—the periodic Anderson model (PAM)—in which the occupation is restricted between $n_f = 1$ (f^1) and $n_f = 0$ (f^0), and a consensus has been developed that the exotic phenomena such as non-Fermi liquid (NFL) and heavy fermion superconductivity (SC) in the vicinity of the quantum critical point (QCP) are mediated by spin fluctuations. Besides, recent discoveries of the maximum in the SC critical temperature at rather higher pressure P_C than the pressure-tuned magnetic QCP [1–4] lead to the discussion of a second quantum mechanism, the possibility of SC pairs being mediated by critical valence fluctuations. A theoretical study in the multiband PAM on the influence of the crystalline electric field (CEF) splitting by Ikeda *et al* [5] indicates that, in the case where the CEF ground state is in an $n_f = 2$ (f^2) singlet, the quasiparticle contribution to the susceptibility is unenhanced, while the density of states (DOS) at the Fermi level E_F of the quasiparticles is enhanced, producing the heavy fermions. The T^2 resistivity coefficient A drastically decreases in magnitude

[4] Present address: International Innovation Center, Kyoto University, Kyoto 606-8502, Japan.

around P_C, indicating that the mass enhancement due to the spin correlation is quickly lost. The so-called Kadowaki–Woods (KW) ratio A/γ^2 [6], where γ is the Sommerfeld coefficient of the electronic specific heat, quickly crosses over from that of the strongly correlated class to a weakly correlated one.

In this paper we report on the quantum criticality of the ytterbium-based compounds—$YbAuCu_4$ and the related compounds—with noninteger valence between the hole occupations $n_f = 1$ (f^{13}) and $n_f = 0$ (f^{14}), investigated through the electrical resistivity, magnetization, and nuclear spin–lattice relaxation rate measurements as a function of applied magnetic field H. $YbAuCu_4$ crystallizes in a cubic $AuBe_5$ (C15b type) structure and has hole occupation close to unity ($n_f = 0.95$ at 300 K [7]). Yb and Au atoms sit on distinct face centred cubic sublattices at (0, 0, 0) (4a site) and (1/4, 1/4, 1/4) (4c site), and are surrounded by space-filling Cu tetrahedra centred at (3/4, 3/4.3/4) (16e site). The inelastic neutron scattering measurements revealed the Γ_7 doublet as the CEF ground state, followed by a Γ_8 quartet, 3.89 meV above it [8]. The compound exhibits the antiferromagnetic (AFM) order below $T_N \simeq 0.9$ K with an incommensurate propagation vector, and the ordered magnetic moment $\simeq 0.85\ \mu_B$/Yb is smaller than $\langle\mu_{\Gamma_7}\rangle = g_J\mu_B\langle\Gamma_7|J_z|\Gamma_7\rangle = 1.71\mu_B$ of the ground state Γ_7 (doublet) [9]. The low-temperature specific heat measurement yielded a rather large Sommerfeld coefficient, $\gamma \sim 2$ J mol^{-1} K^{-2} [10], leading us to place the compound close to the HFL regime with a narrow *cf* hybridized band near the Fermi level. However, the KW ratio does not belong to the strongly correlated class with doublet orbital degeneracy ($N = 2$),[5] but rather the weakly correlated one with $N = 8$, as many ytterbium-based HFL compounds do [12]. On the other hand, the magnetic properties at low temperatures have been ascribed to dominant Ruderman–Kittel–Kasuya–Yosida interactions between incompletely Kondo compensated moments.

Experimental details, results, and the data analyses are reported in section 2, which provide clear evidence that with the application of external magnetic field H, $YbAuCu_4$ is driven from the originally AFM ordered ground state to a nonmagnetic Fermi liquid one through the field-tuned QCP at $H_{cr} \simeq 13$ kOe. The experimental results also provide the first evidence that a crossover valence transition near the magnetic QCP is stabilized with field. In section 3, we report the T–H phase diagram of $YbAuCu_4$ and the T–X phase diagram established for the $YbXCu_4$ (X = Pd, Au, Cu, and Ag) series, which indicate that the evolution of valence fluctuations near the magnetic QCP quickly interacts with the critical spin fluctuations. We attempt to place the implication of present experimental results: the competition between the Kondo temperature and crossover valence transition temperature is central to the long-standing puzzles of localized–itinerant duality and the extent of degeneracy in the crystal electric field ground state.

[5] A preliminary resistivity and NMR/NQR study on $YbAuCu_4$ was briefly reported in [11].

2. Experimental details, results, and data analyses

Polycrystalline samples were synthesized by slow-cooling stoichiometric ratios of the constituent elements in a sealed Ta tube.

2.1. Electrical resistivity

The AC electrical resistivity ρ measured at low temperatures down to 55 mK in several fixed fields H is plotted in figure 1(a). The solid curve (ρ_{ph}) drawn for 40 kOe is the best fit with the ρ data in the range 7–10 K and below 1.35 K. Figure 1(b) shows the temperature dependence of $\rho - \rho_{ph}$ for each of the fields. Upon cooling, the magnetic resistivity $\rho_{mag} = \rho - \rho_{ph}$ displays a logarithmic increase followed by a clear local maximum at $T_0^{(\rho)}$ ($\sim$1.5 K in zero field). The rapid decrease of ρ_{mag} below $T_0^{(\rho)}$ can be ascribed to the coherent Kondo scattering below T_K, or the valence transition below T_V. In figure 1(c), the ρ data at low temperatures are plotted against T^2. Each of the ρ data in different fields is appropriately shifted along the vertical axis. The straight lines drawn in the figure are the best fit of $\rho = \rho_0 + AT^2$ with the corresponding data, and the large prefactors A ($\simeq 4\ \mu\Omega$ cm K^{-2} in zero field) are indicative of the scattering of heavy electrons below an onset temperature $T_{FL}^{(\rho)}$. The $d\rho/dT$ versus T plots shown in figure 1(d) have a local maximum at $T_N^{(\rho)}$, yielding an estimate of the AFM ordering temperature ($\sim$0.9 K in zero field [10, 13]).

The field dependences of $T_0^{(\rho)}$, $T_{FL}^{(\rho)}$, and $T_N^{(\rho)}$ extracted from the ρ data are plotted in figure 2 by blue filled squares, red crosses, and green filled squares, respectively. With increasing H, $T_N^{(\rho)}$ shifts toward lower temperatures and approaches zero at a critical field $H_{cr} \simeq 13$ kOe. In the vicinity of the magnetic to nonmagnetic transition at H_{cr}, the onset temperature $T_{FL}^{(\rho)}$ of the Landau Fermi liquid state exhibits a local minimum. The T^2 resistivity coefficient A plotted by red open circles in figure 3 against H on a semi-log scale displays a shoulder peak around H_{cr} followed by a rapid decrease. Shown in figure 4 is the field dependence of DC resistivity observed at the lowest temperature 55 mK of the experiment. The small residual resistivity $\rho_0 \simeq 4.5\ \mu\Omega$ cm at 50 kOe indicates the high quality of the investigated polycrystalline sample. With increasing H, ρ_0 also displays a maximum in the vicinity of H_{cr} followed by a monotonic decrease. These features strongly suggest that with the application of external magnetic field, $YbAuCu_4$ is driven from the AFM ordered ground state to a nonmagnetic Fermi liquid one through the field-tuned QCP in the vicinity of $H_{cr} \simeq 13$ kOe [14], whereas $T_0^{(\rho)}$ of the ρ maximum is initially insensitive to H, and exhibits a significant increase in fields above $\sim H_{cr}$.

2.2. Magnetization

The magnetization M was measured in a temperature range between 1.5 and 40 K at several fixed fields, and the data divided by H are plotted in figure 5 against temperature on a log–log scale. Upon cooling, M/H in the lowest field 5 kOe of the present experiment displays a Curie–Weiss (CW) type

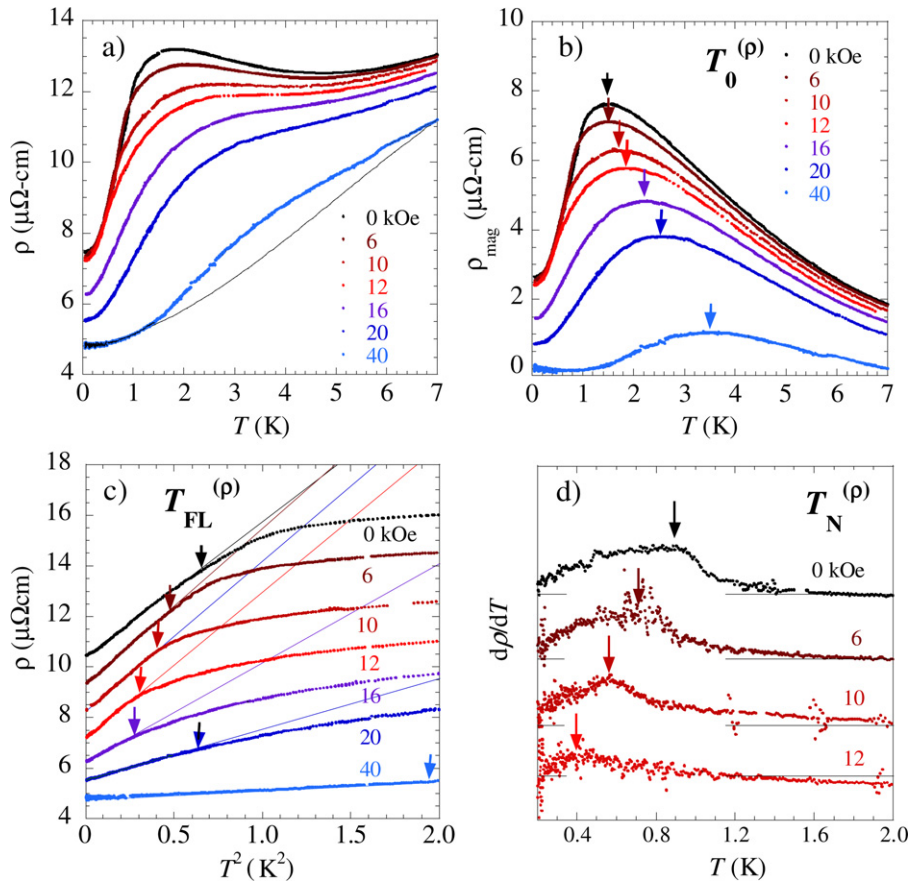

Figure 1. (Colour online) (a) AC electrical resistivity ρ of a $YbAuCu_4$ polycrystalline sample plotted against T in a range between 0.055 and 7 K at several fixed fields. The solid curve drawn for 40 kOe is the best fit with the ρ data in a range 7–10 K and below 1.35 K. (b) ρ_{mag} obtained by subtracting the broken curve drawn in (a). (c) ρ versus T^2 plots at low temperatures. Each of the ρ data in different fields is appropriately shifted along the vertical axis. Solid lines are the best fit of $\rho = \rho_0 + AT^2$ with the corresponding data. (d) $d\rho/dT$ versus T plots. T_N at the local maximum indicated by arrows gives an estimate of the Néel temperature.

increase (red broken curve) down to ∼1.5 K and, therefore, the uniform susceptibility χ can be defined by M/H. With increasing H, M/H tends to exhibit saturating behaviour at low temperatures well below $T_0^{(\rho)}$ (temperature of the ρ maximum, indicated by a filled arrow) and $T_0^{(T_1)}$ (temperature of the $1/T_1T$ maximum described later on, indicated by an open arrow). The M plateau at low temperatures indicates that $YbAuCu_4$ takes a Pauli paramagnetic ground state in high fields. The field dependence of M at 1.5 K plotted in the inset suggests that M at low temperatures is monotonically enhanced with increasing H, which is consistent with the field dependence of M measured at a lower temperature of 0.5 K by Bauer *et al* [10].

2.3. Nuclear spin–lattice relaxation rate

Measurements of the nuclear spin–lattice relaxation rate $1/T_1$ reveal the spin-fluctuation character from the q averaged dynamical spin susceptibility $\chi(\vec{q}, \omega)$,

$$1/T_1 = \frac{k_B \gamma_n T}{2\mu_B^2} \Sigma_q A_{hf}(q)^2 \,\mathrm{Im}\,\chi(\vec{q}, \omega)/\omega_N. \qquad (1)$$

Here, $\vec{q}$ is the wavevector of the spin fluctuations, ω_N the resonance frequency, and $A_{hf}(q = 0)/\gamma_n\hbar$ the hyperfine field on a given nucleus given by the magnetic moment of neighbouring f electrons. We have carried out the nuclear quadrupole resonance (NQR) and nuclear magnetic resonance (NMR) of ^{63}Cu ($I = 3/2$) on the 16e site at low temperatures down to 80 mK in several fixed fields from zero up to 110 kOe. The NMR and NQR signals were observed by using wide-band phase-coherent pulsed spectrometers.

Because of the noncubic local symmetry at 16e sites, a single ^{63}Cu NQR line is observed in zero field at frequencies around 8.96 MHz. T_1 was measured at the peak intensity point. The magnetization recovery data $M(t)$ at time t after the initial single saturation pulse show a single-exponential behaviour as shown in figure 6(a). The value of T_1 is deduced by fitting the relation

$$[M(\infty) - M(t)]/M(\infty) = e^{-3t/T_1} \qquad (2)$$

with the recovery data.

The NMR spectrum observed by a field-sweeping procedure is a superposition of ^{63}Cu and ^{65}Cu ($I = 3/2$) quadrupolar-split powder-pattern spectra, each of which consists of a central line and a satellite pair. The Knight shift K of ^{63}Cu on the 16e site was deduced from the well discriminated ^{63}Cu central line at $\omega_N = 75$ MHz and high

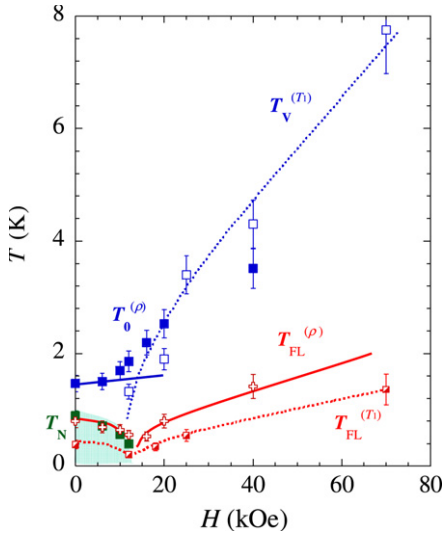

Figure 2. (Colour online) (a) T–H phase diagram of $YbAuCu_4$. $T_{FL}^{(\rho)}$ (red crosses), $T_0^{(\rho)}$ (blue filled squares), and $T_N^{(\rho)}$ (green filled squares) are temperatures of the onset of T^2 resistivity (ρ) and maxima of ρ and $d\rho/dT$, respectively. $T_{FL}^{(T_1)}$ (red squares), $T_V^{(T_1)}$ (blue open squares) and $T_N^{(T_1)}$ (green open squares) are temperatures of the onset of Korringa-like relaxation behaviour ($1/T_1T$ = const.), and the maximum and kink in $1/T_1T$, respectively. Each of the dashed curves drawn in the figure is a guide to the eye for corresponding data.

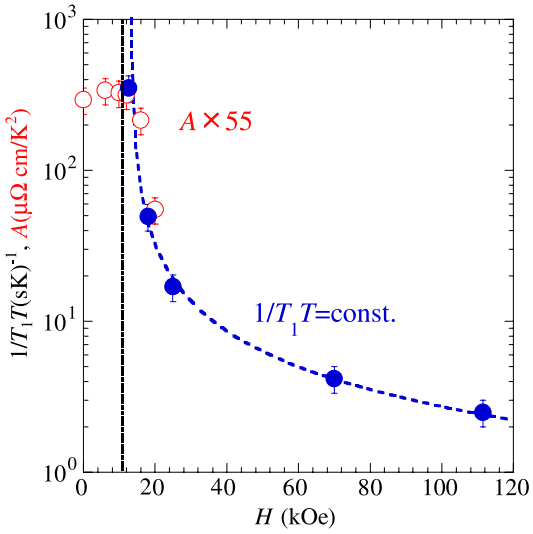

Figure 3. (Colour online) Field dependence of the T^2 resistivity coefficient A (red open circles) and the value of the $1/T_1T$ plateau (blue filled circles) in the Fermi liquid state of $YbAuCu_4$ at low temperatures. The dashed curve is the best fit of $1/T_1T \propto (H - H_{cr})^{-1}$ with the data in fields above $H_{cr} \simeq 13$ kOe.

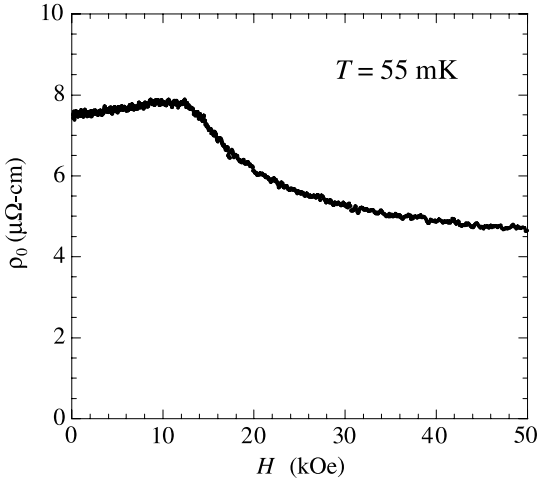

Figure 4. Field dependence of the DC resistivity of $YbAuCu_4$ at a fixed temperature, 55 mK.

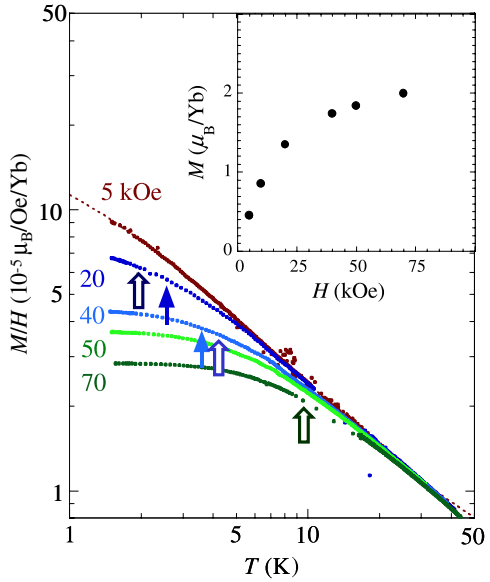

Figure 5. (Colour online) Temperature dependence of the magnetization M of $YbAuCu_4$ divided by magnetic field H. The red broken curve is the best fit of the Curie–Weiss law with the data at 5 kOe. Filled and open arrows indicate $T_0^{(\rho)}$ of the ρ maximum and $T_V^{(T_1)}$ of the $1/T_1T$ maximum in corresponding fields. The inset displays the field dependence of magnetization at 1.5 K.

temperatures above 50 K, and the K versus χ plots yield the hyperfine field $A_{hf}(q = 0)/\gamma_n\hbar \simeq -0.63$ kOe/μ_B [15].

Because of the large linewidth broadening at low temperatures, the ^{65}Cu upper satellite line partly superposes on the ^{63}Cu central line at resonance frequencies above 25 MHz as typically shown in figure 7(a). T_1 was not measured at the ^{63}Cu central line, but the ^{63}Cu upper satellite line (indicated by the open arrow in the figure). This is to avoid the effect of superposition on the central line of the ^{65}Cu upper satellite line and/or a possible spurious NMR signal originating from a small amount of Cu on the 4c sites due to site disorder. The multi-exponential behaviour of $M(t)$ after the initial single saturation pulse[6] (typically shown in figure 6(c)) is well

[6] In the case of nonequally separated nuclear spin levels, the recovery behaviour of the magnetization is very sensitive to the initial saturation condition imposed on the nuclear spin levels. We applied the single saturation pulse that makes the initial population on each of the spin levels clear, making the fitting of theoretically calculated recovery curve with the recovery data reliable.

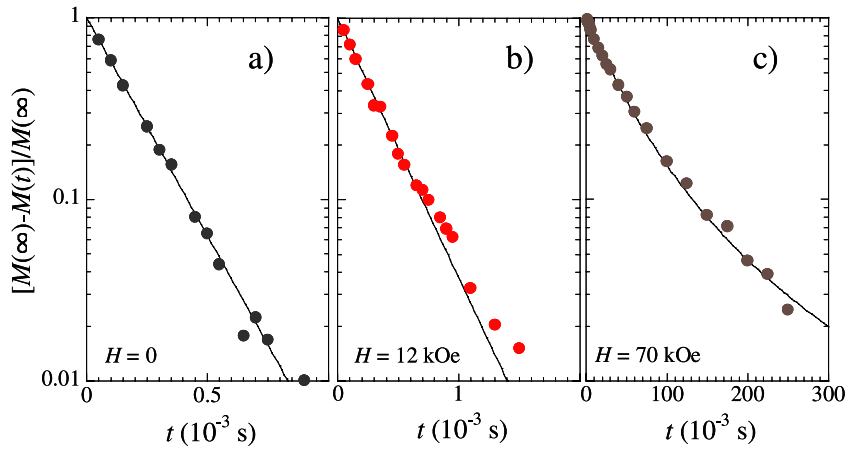

Figure 6. (Colour online) Magnetization recovery behaviour of ^{63}Cu in $YbAuCu_4$ at 1.35 K observed in fields (a) 0 kOe (NQR), (b) 12 kOe (NMR), and (c) 70 kOe (NMR), respectively, after the initial single saturation pulse. The solid lines are the best fit of the theoretically calculated recovery curves described in the text with the corresponding data.

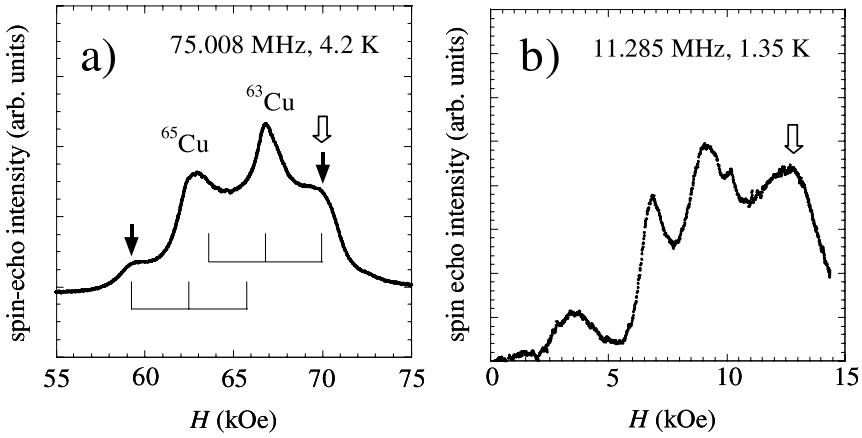

Figure 7. ^{63}Cu and ^{63}Cu NMR spectrum in $YbAuCu_4$ observed by field-sweeping procedure: (a) 75.01 MHz at 4.2 K; (b) 11.285 MHz at 1.35 K. The spin lattice relaxation time T_1 is measured at the resonance peak indicated by open arrows.

reproduced by the relation

$$\frac{M(\infty)-M(t)}{M(\infty)} = 0.1\mathrm{e}^{-t/T_1} - 0.5\mathrm{e}^{-3t/T_1} - 0.4\mathrm{e}^{-6t/T_1} \quad (3)$$

for the NMR satellite line [16].

In a low field, $H = 12$ kOe, the Zeeman and the quadrupole interactions are of the same order of magnitude, resulting in a rather complex NMR spectrum in shape, as shown in figure 7(b). T_1 was measured at the resonance peak indicated by the open arrow in the figure. The $M(t)$ data shown in figure 6(b) cannot be reproduced by either the single-exponential or the multi-exponential behaviour described above. We have numerically calculated the rate equations for the mixed nuclear spin levels, and obtained the magnetization recovery behaviour

$$\frac{M(\infty)-M(t)}{M(\infty)} = 0.058\,\mathrm{e}^{-5.11t/T_1} + 0.116\,\mathrm{e}^{-4.79t/T_1} + 0.826\,\mathrm{e}^{-3.99t/T_1} \quad (4)$$

for the corresponding transition with angle $\theta = \pi/2$ between the field and quadrupole principal axis. The recovery data are rather well reproduced by this relation. The small deviation is considered to be caused by the small overlapping of distinct resonance lines.

Figure 8 shows the $1/T_1T$ data plotted against temperature in a range between 0.08 and 50 K on a log–log scale. Upon cooling in zero field, $1/T_1T$ exhibits a marked increase in proportion to $T^{-4/3}$ down to $\sim$1 K, being larger than the CW type increase expected from the experimental χ (black solid line in the figure). This result indicates a significant increase of $\chi(\vec{q})$ with $\vec{q} \neq 0$. The sharp $1/T_1T$ peak at $\sim$1 K accompanied by markedly large broadening of NQR linewidth is ascribed to the AFM ordering. The important feature is that, at low temperatures well below T_N, $1/T_1T$ becomes nearly constant, instead of the rapid drop associated with the freezing of the AFM spin fluctuations. This result reveals that in zero field $YbAuCu_4$ is in the Fermi liquid state. In fields well above H_{cr}, $1/T_1T$ at high temperatures follows the CW law ($1/T_1 \simeq$ const.); the relaxation is dominated by the localized electron spin fluctuations. Upon cooling, $1/T_1T$ begins to deviate from the CW law, takes a broad maximum around $T_V^{(T_1)}$, and exhibits a large decrease followed by a

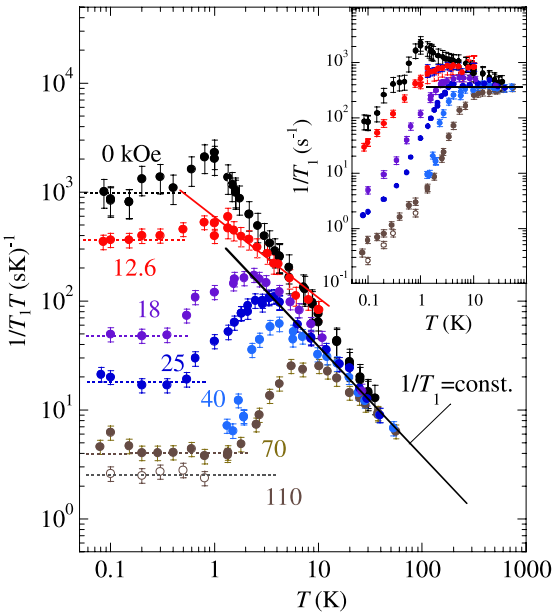

Figure 8. Temperature dependence of the ^{63}Cu spin–lattice relaxation rate $1/T_1$ divided by T in $YbAuCu_4$ at several fixed fields. The solid black line represents the $1/T_1$ = const. relation, and the solid red line the relation $1/T_1 \propto T^{-3/4}$. Horizontal dashed lines for the $1/T_1T$ plateau at low temperatures are drawn as guides to the eye. The inset shows the $1/T_1$ data.

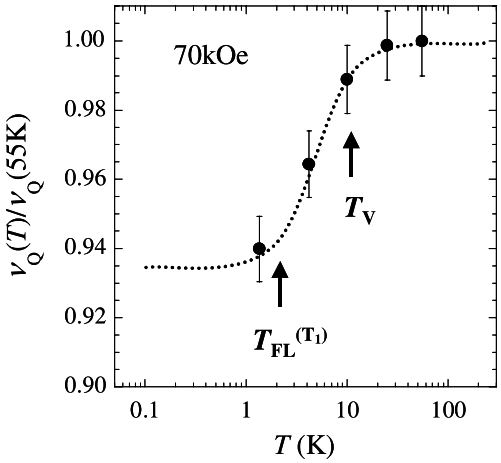

Figure 9. Temperature dependence of the quadrupole frequency ν_Q. The dashed curve is a guide to the eye.

$1/T_1T$ plateau at low temperatures below $T_{FL}^{(T_1)}$. The large $1/T_1T$ decrease below $T_V^{(T_1)}$ cannot be explained by a possible slowing down of spin fluctuations, because the ^{63}Cu NMR does not exhibit significant anomalies either in the Knight shift or the linewidth.

Figure 9 shows the temperature dependence of nuclear quadrupole frequency ν_Q at 70 kOe, extracted from the interval between the upper satellite line of the ^{63}Cu NMR spectrum and the lower one of the ^{65}Cu spectrum (indicated by solid arrows in the inset of figure 7(a)). The significant decrease of ν_Q observed below $\sim T_V^{(T_1)}$ provides evidence for the expansion of unit-cell volume ($\propto 1/\nu_Q$). A similar broad $1/T_1T$ maximum accompanied by volume expansion has been observed in the NQR study on the related nonmagnetic HFL compound $YbAgCu_4$ with noninteger valence[7], whereas there is a sharp $1/T_1T$ peak in the prototypical first-order valence transition compound $YbInCu_4$ [15]. It has been rather elusive whether the $1/T_1T$ and/or χ peaks observed for $YbAgCu_4$ around 40 K originate from the Kondo effect or the valence transition. It was initially claimed that the χ data can be fitted quantitatively to the numerical predictions of the $J = 7/2$ Coqblin–Schrieffer model (CSM), although the characteristic temperature is rather lower than the Kondo temperature $T_K \sim 100$ K extracted from fits to various low-temperature physical properties. However, later measurements of x-ray diffraction provide clear evidence for the volume expansion below ~40 K, strongly suggesting a crossover valence transition. In the $YbAuCu_4$ case of the present study, the extremely large $1/T_1T$ decrease below $\sim T_V^{(T_1)}$ observed in high fields cannot be reproduced by the CSM at all. The volume expansion extracted from the change in ν_Q reasonably leads to a conclusion that the crossover valence transition takes place at temperatures near the $1/T_1T$ maximum. With decreasing H, $T_V^{(T_1)}$ shifts toward lower temperatures and the value of the $1/T_1T$ plateau is greatly enhanced. Similar $T_V^{(T_1)}$ suppression and the enhancement of $1/T_1T$ = const. were observed in the nonmagnetic HFL $YbCu_5$ on the way to getting closer to the QCP with the application of pressure [17].

The field dependences of the crossover valence transition temperature $T_V^{T_1}$, onset temperature of Fermi liquid $T_{FL}^{(T_1)}$, and AFM ordering temperature $T_N^{(T_1)}$ extracted from the $1/T_1T$ data are plotted in figure 2 by blue open squares, red squares, and green open squares, respectively. The lower $T_{FL}^{(T_1)}$ than $T_{FL}^{(\rho)}$ is considered to be caused by their different definitions. The values of $1/T_1T$ = const. at low temperatures below $T_{FL}^{(T_1)}$ are also plotted in figure 3 by blue filled circles. It is worth noting that both $1/T_1T$ and A in the Fermi liquid state are proportional to the square of the DOS, $N(E_F)^2$, at E_F. The plots in fields above $H_{cr} \sim 13$ kOe are well reproduced by the relation $1/T_1T \propto (H - H_{cr})^{-1}$, indicating that the effective mass m^* of quasiparticles is greatly enhanced in the vicinity of H_{cr}. This result provides microscopic evidence for the field-tuned QCP in $YbAuCu_4$.

3. Discussion

3.1. Field-tuned QCP

Figure 2 shows the T–H phase diagram of $YbAuCu_4$ extracted from the ρ and T_1 data of the present study. With the application of external magnetic field, the compound can be tuned to the QCP at $H_{cr} \simeq 13$ kOe (continuous transition from magnetic to nonmagnetic states at $T = 0$). However, the onset temperature of the Fermi liquid state $T_{FL}^{(T_1)}$ ($T_{FL}^{(\rho)}$) takes the local minimum, but remains finite, indicating that the compound at low temperatures is in the HFL state in all experimental fields. In other words, m^* is greatly enhanced in the vicinity

[7] The volume expansion in $YbAgCu_4$ below ~50 K was detected by x-ray diffraction measurements; unpublished.

of the QCP, but there is not a divergent increase. These features are similar to the T^2 resistivity behaviour reported for $YbRh_2Si_2$ [18], that has been intensively investigated as one NFL material among the stoichiometric Yb-based compounds [18–20]. The temperature and magnetic field participating in the NFL-like phenomena in the vicinity of the field-driven QCP of $YbAuCu_4$ are about one order higher in energy than those of $YbRh_2Si_2$. This is acceptable if one takes the difference in the AFM transition temperature into consideration: $T_N \sim 0.9$ K for $YbAuCu_4$ and ~0.07 K for $YbRh_2Si_2$, respectively.

3.2. Competition between valence and spin fluctuations

The most important feature in figure 2 is that $T_V^{(T_1)}$ defined at the $1/T_1T$ maximum rapidly decreases to zero with the decrease of H close to H_{cr}, and completely disappears in the AFM ordered state in low field below H_{cr}. On the other hand, with the application of H, $T_0^{(\rho)}$ defined at the ρ maximum initially displays nearly field-independent behaviour, and a significant increase for fields above H_{cr}. Here, it is important to point out that both the coherent Kondo scattering at T_K and the crossover valence transition at T_V are able to yield the ρ maximum. Thus, it is reasonable to ascribe the initial field-independent $T_0^{(\rho)}$ to the Kondo effect (T_K), and the field-dependent $T_0^{(\rho)}$ in high fields above H_{cr} to the crossover valence transition (T_V). Upon cooling in low fields ($<H_{cr}$) $YbAuCu_4$ initially transforms into the HFL state below $T_K \simeq 1.5$ K, and displays the AFM order below T_N, whereas in fields well above H_{cr} the compound initially displays the field-induced crossover valence transition at T_V, and transforms into the Fermi liquid state at low temperatures below $T_{FL}^{(\rho)}$. Figure 2 provides the first experimental evidence that the crossover valence transition in the vicinity of QCP is stabilized with the application of H, in contrast to the destabilization of the first-order valence transition. This result is consistent with the recent theoretical scenario of 'magnetic field control of valence transition' using the extended PAM by Watanabe and Miyake [21].

In fields close to H_{cr}, the Kondo interaction (k_BT_K) competes with the valence transition (k_BT_V) in energy. As can be seen in figure 2, in a field of 12.6 kOe close to H_{cr}, the development of AFM spin fluctuations observed in zero field is largely suppressed, and the $1/T_1T$ data below ~7 K tend to follow the power-law relation $1/T_1T \propto T^{-3/4}$ (red line in the figure) that is one of the theoretically predicted NFL phenomena at the AFM QCP [22]. However, $1/T_1T$ at lower temperatures displays a very small broad maximum around 1 K instead of continuing the power-law increase, and exhibits the $1/T_1T$ plateau below ~0.4 K. The NMR spectrum did not exhibit any significant linewidth broadening below ~1 K, consistent with the complete suppression of AFM order in this field. Thus, the unconventional behaviour of $1/T_1T$ in the vicinity of H_{cr} suggests that the development of quantum critical spin correlation is being limited by remnants of the valence fluctuations. The KW ratio A/γ^2 of $YbAuCu_4$ belongs to the weakly correlated class with orbital degeneracy $N = 8$, in spite of the Γ_7 CEF ground state ($N = 2$). The

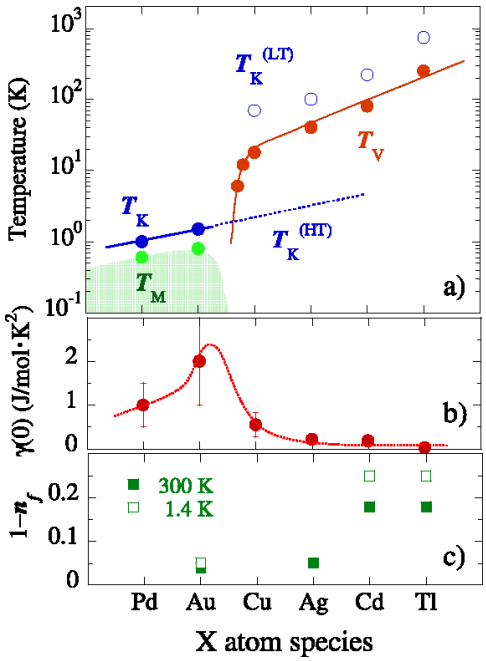

Figure 10. (Colour online) Schematic phase diagram of the $YbXCu_4$ series. (a) X dependence of T_K (blue circles), T_V (red circles), and T_M (green circles) cited in the text. (b) X dependence of specific coefficient $\gamma(0)$. (c) X dependence of occupation number $1 - n_f$ of 4f electrons in the Yb^{3+} hole band.

experimental γ consists essentially of two terms: γ_{cor} due to the spin correlation effect, and γ_{band} to the band effect. γ_{cor} and A are related to each other through the Kramers–Krönig relation, generally leading to the large value of KW ratio [23]. The loss of γ_{cor} caused by the valence fluctuations reduces the value of A/γ^2, leading $YbAuCu_4$ and many of the ytterbium-based compounds with doubly degenerate CEF ground state to the rather weakly correlated class.

Finally, we established a schematic phase diagram of the $YbXCu_4$ series except the first-order valence transition compound $YbInCu_4$. Three characteristic temperatures T_K, T_V, and T_M (T_N or T_C) are plotted in figure 10(a) against the compounds placed in order of the magnitude of T_K. Here T_V is defined by the local maximum in χ [7], or $1/T_1T$ [15, 17], or ρ [24]. γ and $1 - n_f$ [7, 9] are plotted in figures 10(b) and (c), respectively. In the nonmagnetic compounds (X = Cu, Ag, Cd, Tl), no Kondo anomaly has been observed around $T_K^{(LT)}$ ($\gg T_V$) that was extracted from the low-temperature susceptibility data [7]. This result leads to a consideration that, in the compounds with crossover valence transition, $T_K^{(HT)}$ expected in the high-temperature localized 4f electron state is much lower than T_V. Upon cooling, the compounds initially display the crossover valence transition at T_V, and transform into the HFL state characterized by the values of $T_K^{(LT)}$ and γ extracted from the physical properties at low temperatures.

The phase boundary between magnetic and nonmagnetic regimes is located in the middle of $YbAuCu_4$ and $YbCu_5$ (figure 10(a)), where γ takes the local maximum (figure 10(b)). The important feature in this phase diagram is that in the vicinity of the phase boundary, T_V crosses the linear extrapolation of T_K of the magnetic compounds (X = Pd

and Au), and approaches zero. This feature indicates that at the pressure-tuned QCP the nonmagnetic compounds would display unconventional quantum critical phenomena caused by the competition between T_K and T_V similar to those observed at the field-tuned QCP of magnetic $YbAuCu_4$.

As can be seen in figures 10(a)–(c), T_V of the nonmagnetic compounds rises with the increase of $1 - n_f$. The larger extent of one-electron fluctuation between the localized 4f orbital and itinerant 5d states in the ytterbium case than in the cerium case is considered to make the valence transition more stable, and the strong spin correlations emerge only in the small mixed-valence region ($n_f \neq 1$, but close to unity). These results lead to a band scheme of a weakly broadened 4f hole level above the Fermi sea and the partial DOS extends to the Fermi level. In the nonmagnetic compounds with large mixed valence (X = Cu, Ag, Cd, Tl), the magnetic susceptibility χ displays the local maximum at temperatures in the vicinity of T_V [7].

However, as shown in figure 5, M/H of $YbAuCu_4$ in high fields does not display the local maximum, but a saturating behaviour at low temperatures well below $T_V^{(T1)}$ (indicated by open arrows). The strong localized–itinerant duality observed in $YbAuCu_4$ and $YbPdCu_4$ [10] is reasonably explained by this band scheme: the magnetic susceptibility characteristic of the dense Kondo effect is ascribed to the narrow 4f band; and the electrical resistivity and nuclear spin–lattice relaxation rate characteristic of itinerant electrons to the cf hybridized band near the Fermi level.

4. Conclusion

We have reported the electrical resistivity, magnetization, and NMR and NQR studies on the quantum criticality of $YbAuCu_4$ with noninteger valence close to unity. With increasing H, $YbAuCu_4$ is driven from the originally AFM ordered ground state ($T_N \sim 0.9$ K) to a nonmagnetic Fermi liquid one through the field-tuned QCP at $H_{cr} \simeq 13$ kOe. The experimental results also provide the first evidence that a crossover valence transition near the magnetic QCP is stabilized with the application of external magnetic field, in marked contrast to the destabilization of the first-order valence transition. The T–H phase diagram of $YbAuCu_4$ and the T–X phase diagram established for the $YbXCu_4$ (X = Pd, Au, Cu, Ag) series indicate that the evolution of valence fluctuations near the magnetic QCP quickly interacts with the critical spin fluctuations. We have suggested that the competition between the Kondo temperature and crossover valence transition temperature is central to the long-standing puzzles of localized–itinerant duality and the extent of degeneracy in the crystal electric field ground state.

Acknowledgments

The authors wish to express their thanks to Professor T C Kobayashi, Dr H Kotegawa and Mr K Tabira (Okayama University) for the electrical resistivity measurements at low temperatures, and to Professor M Sera (Hiroshima University) for the magnetization measurements at several fixed fields. Thanks are also due to Mr Y Ihara and Mr Y Nakai (Kyoto University) for helping with the T_1 measurements at low temperatures. The authors also wish to express their thanks to Professor K Miyake and Dr S Watanabe for valuable discussions. One of the authors (AY) has been supported by the Japan Society for the Promotion of Science for Young Scientists.

References

[1] Onishi Y and Miyake K 2000 *J. Phys. Soc. Japan* **69** 3955
[2] Jaccard D, Wilhelm H, Alami-Yadri K and Vargoz E 1999 *Physica* B **259–261** 1
Holmes A T, Jaccard D and Miyake K 2004 *Phys. Rev.* B **69** 024508
[3] Sidorov V A *et al* 2002 *Phys. Rev. Lett.* **89** 157004
[4] Kawasaki S, Zheng G-q, Kan H, Kitaoka Y, Shishido H and Onuki Y 2005 *Phys. Rev. Lett.* **94** 037007
[5] Ikeda H and Miyake K 1997 *J. Phys. Soc. Japan* **66** 3714
[6] Kadowaki K and Woods S B 1986 *Solid State Commun.* **58** 507
[7] Sarrao J L, Immer C D, Fisk Z, Booth C H, Figueroa E, Lawrence J M, Modler R, Cornelius A L, Hundley M F, Kwei G H, Thompson J D and Bridges F 1999 *Phys. Rev.* B **59** 6855
[8] Severing A, Murani A P, Thompson J D, Fisk Z and Loong C K 1990 *Phys. Rev.* B **41** 1739
[9] Bauer E, Fisher P, Marabelli F, Ellerby M, McEwan K A, Roessili B and Fernandes-Dias M T 1997 *Physica* B **234–236** 676
[10] Bauer E, Gratz E, Hauser R, Tuan Le, Galatanu A, Kottar A, Michor H, Perthold W, Hilscher G, Kagayama T, Oomi G, Ichimiya N and Endo S 1994 *Phys. Rev.* B **50** 9300
[11] Yamamoto A, Wada S and Sarrao J L 2007 *J. Phys. Soc. Japan (Letter)* **76** 063709
[12] Tsujii N, Kontani H and Yoshimura K 2005 *Phys. Rev. Lett.* **94** 057201
[13] Nakamura H, Shiga M, Kitaoka Y, Asayama K and Yoshimura K 1996 *J. Phys. Soc. Japan* **65** (suppl. B) 168
[14] Yamamoto A, Wada S and Sarrao J L 2007 *J. Phys. Soc. Japan* **76** 063709
[15] Koyama T, Matsumoto M, Tanaka T, Ishida H, Mito T, Wada S and Sarrao J L 2002 *Phys. Rev.* B **66** 4302
[16] For example, MacLaughlin D E *et al* 1971 *Phys. Rev.* B **4** 60
[17] Mito T *et al* 2008 in preparation
[18] Knebel G, Boursier R, Hassinger E, Lapertot G, Niklowitz P G, Pourret A, Salce B, Sanchez J P, Sheikin I, Bonville P, Harima H and Flouquet J 2006 *J. Phys. Soc. Japan* **75** 114709
[19] Ishida K, Okamoto K, Kawasaki Y, Kitaoka Y, Trovarelli O, Geibel C and Steglich F 2002 *Phys. Rev. Lett.* **89** 107202
[20] Custers J, Gegenwart P, Neumaier K, Wilhelm H, Oeschler N, Ishida K, Kitaoka Y, Geibel C and Steglich F 2003 *J. Phys.: Condens. Matter* **15** S2047–53
[21] Watanabe S, Tsuruta A, Miyake K and Flouquet J 2008 *Phys. Rev. Lett.* submitted
[22] Moriya T and Takimoto T 1995 *J. Phys. Soc. Japan* **64** 960
[23] Miyake K, Matsuura T and Varma C M 1989 *Solid State Commun.* **71** 1149
[24] Galli M, Bauer E, Berger St, Dusek Ch, Della Mea M, Michor H, Kaczorowski D, Scheidt E W and Marabelli F 2002 *Physica* B **312/313** 489